Lenia: Biology of Artificial Life

Bert Wang-Chak Chan
Hong Kong

A new system of artificial life called *Lenia* (from Latin *lenis* "smooth"), a two-dimensional cellular automaton with continuous spacetime state and generalized local rule, is reported. Computer simulations show that Lenia supports a great diversity of complex autonomous patterns or "life forms" bearing resemblance to real-world microscopic organisms. More than 400 species in 18 families have been identified, many discovered via interactive evolutionary computation. They differ from other cellular automata patterns in being geometric, metameric, fuzzy, resilient, adaptive and rule generic.

Basic observations of the system are presented regarding the properties of spacetime and basic settings. A broad survey of the life forms is provided and categorized into a hierarchical taxonomy, and their distribution is mapped in the parameter hyperspace. Their morphological structures and behavioral dynamics are described, and possible mechanisms of their self-organization, self-direction and plasticity are proposed. Finally, the study of Lenia and how it would be related to biology, artificial life and artificial intelligence is discussed.

Keywords: artificial life; geometric cellular automata; complex system; interactive evolutionary computation

1. Introduction

Among the long-term goals of artificial life are to simulate existing biological life and to create new life forms using artificial systems. These are expressed in the 14 open problems in artificial life [1], in which number three is of particular interest here:

> Determine whether fundamentally novel living organizations can exist.

There have been numerous efforts to create and study novel mathematical systems that are capable of simulating complex lifelike dynamics. Examples include particle systems like swarm chemistry [2], primordial particle systems (PPS) [3], reaction-diffusion systems like the U-Skate World [4], cellular automata like the Game of Life (GoL) [5], elementary cellular automata (ECAs) [6], evolutionary systems like virtual creatures [7] and soft robots [8, 9]. These systems have a common theme—let there be countless modules or particles and

https://doi.org/10.25088/ComplexSystems.28.3.251

(often localized) interactions among them, and a complex system with interesting autonomous patterns will emerge, just like how life emerged on Earth 4.28 billion years ago [10].

Life can be defined as the capabilities of self-organizing (morphogenesis), self-regulating (homeostasis), self-directing (motility), self-replicating (reproduction), entropy reduction (metabolism), growth (development), response to stimuli (sensitivity), response to environment (adaptability) and evolving through mutation and selection (evolvability) (e.g., [11–14]). Artificial life systems are able to reproduce some of these capabilities with various levels of fidelity. Lenia, the subject of this paper, is able to achieve many of them, except self-replication, which is yet to be discovered.

Lenia also captures a few subjective characteristics of life, like vividness, fuzziness, aesthetic appeal and the great diversity and subtle variety in patterns that a biologist would have the urge to collect and catalog. If there is some truth in the biophilia hypothesis [15] that humans are innately attracted to nature, it may not be too far-fetched to suggest that these subjective experiences are not merely feelings but among the essences of life as we know it.

Due to similarities between life on Earth and Lenia, we borrow terminologies and concepts from biology, like taxonomy (corresponds to categorization), binomial nomenclature (naming), ecology (parameter space), morphology (structures), behavior (dynamics), physiology (mechanisms) and allometry (statistics). We also borrow spacetime (grid and time step) and fundamental laws (local rule) from physics. With a few caveats, these borrowings are useful in providing a more intuitive characterization of the system and may facilitate discussions on how Lenia or similar systems could give answers to life [16], the universe [17] and everything.

1.1 Background

A *cellular automaton* (CA, plural: cellular automata, CAs) is a mathematical system where a grid of sites, each having a particular state at a moment, is being updated repeatedly according to a local rule and each site's neighboring sites. Since its conception by von Neumann and Ulam [18, 19], various CAs have been investigated, the most famous being Wolfram's one-dimensional elementary cellular automata (ECA) [6, 17] and Conway's two-dimensional Game of Life (GoL) [5, 20]. GoL is the starting point that Lenia came from. It produces a whole universe of interesting patterns [21] ranging from simple "still lifes," "oscillators" and "spaceships" to complex constructs like pattern emitters, self-replicators and even fully operational computers, thanks to its Turing completeness [22].

Several aspects of GoL can be generalized. A discrete *singular* property (e.g., dead-or-alive state) can be *extended* into a range (multi-state), normalized to a *fractional* property in the unit range, and becomes *continuous* by further splitting the range into infinitesimals (real number state). The local rule can be generalized from the basic ECA/GoL style (e.g., totalistic sum) to smooth parameterized operations (weighted sum).

By comparing various CAs that possess autonomous soliton patterns, we observe the *evolution of generalization* with increasing genericity and continuity (Table 1, Figure 1). This suggests that Lenia is currently at the latest stage of generalizing GoL, although there may be room for further generalizations.

♯	System	Type*	Space	Neighborhood	N. Sum
1	ECA, GoL	CA	singular	nearest cube	totalistic
2	continuous ECA	CA	singular	nearest cube	totalistic
3	continuous GoL	EA	continuous	continuous ball	totalistic
4	Primordia	CA	singular	nearest cube	totalistic
5	Larger-than-Life	CA / GCA	fractional	extended cube	totalistic
6	RealLife	EA	continuous	continuous cube	totalistic
7	SmoothLife	GCA	fractional	extended shell	totalistic
8	discrete Lenia	GCA	fractional	extended ball	weighted
9	continuous Lenia	EA	continuous	continuous ball	weighted
♯	References and notes	Growth	Update	Time	State
1	[17, 5]	intervals	replace	singular	singular
2	[17]	mapping	replace	singular	continuous
3	[23]	mapping	replace	singular	continuous
4	†	intervals	replace	singular	extended
5	[24, 25]	intervals	replace	singular	singular
6	[26]	intervals	replace	singular	singular
7	[27]‡	intervals	increment	fractional	fractional
8		mapping	increment	fractional	fractional
9		mapping	increment	continuous	continuous

Table 1. Comparison of genericity and continuity in various CAs. (* GCA = geometrical cellular automata, EA = Euclidean automata, see Section 4. † Primordia is a precursor to Lenia, written in JavaScript/HTML by the author circa 2005. It had multi-states and extended survival/birth intervals. ‡ SmoothLife and Lenia, being independent developments, exhibit striking resemblance in system and generated patterns. This can be considered an instance of “convergent evolution.”)

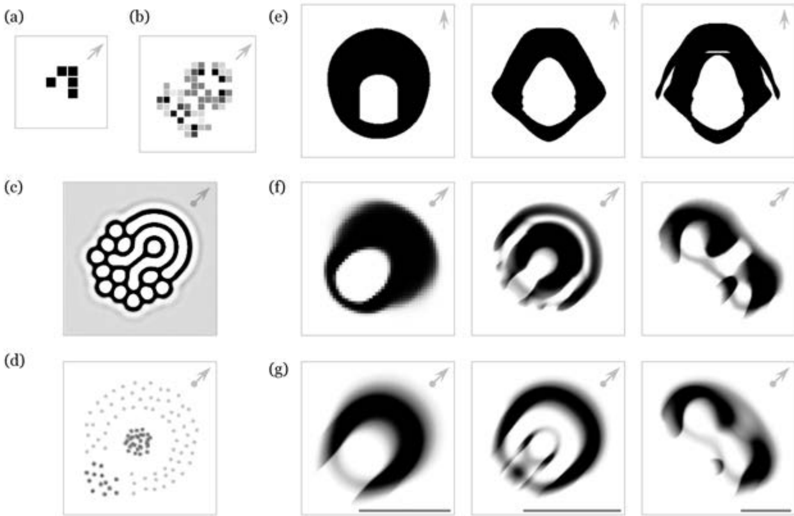

Figure 1. Patterns in artificial life systems: (a–b, e–g) CAs, (c) reaction-diffusion and (d) particle swarm. (↑ = orthogonal; ↗ = diagonal; ⤢ = omnidirectional; scale bar is unit length = kernel radius). (a) GoL: "glider." (b) Primordia: "DX:8/762." (c) U-Skate World: "jellyfish" [28]. (d) Swarm chemistry: "fast walker & slow follower" [29]. (e) Larger-than-life (LtL): "bug with stomach" using ball neighborhood, "bug with ribbed stomach," "bug with wings" [30]. (f) SmoothLife: "smooth glider," "pulsating glider," "wobbly glider" [27, 31, 32]. (g) Lenia: *Scutium*, *Kronium*, *Pyroscutium*.

2. Methods

We describe the methods of constructing and studying Lenia, including its mathematical definition, computer simulation, strategies of evolving new life forms and observational and statistical analysis.

2.1 Definitions

Mathematically, a CA is defined by a 5-tuple (conventionally a 4-tuple with the timeline $\mathcal{T}$ omitted) $\mathcal{A} = \left(\mathcal{L}, \mathcal{T}, \mathcal{S}, \mathcal{N}, \phi\right)$, where $\mathcal{L}$ is the d-dimensional *lattice* or *grid*, $\mathcal{T}$ is the *timeline*, $\mathcal{S}$ is the *state set*, $\mathcal{N} \subset \mathcal{L}$ is the *neighborhood* of the origin, and $\phi : \mathcal{S}^{\mathcal{N}} \to \mathcal{S}$ is the *local rule*.

Define $\mathbf{A}^t : \mathcal{L} \to \mathcal{S}$ as a *configuration* or *pattern* (i.e., collection of states over the whole grid) at time $t \in \mathcal{T}$. $\mathbf{A}^t(\mathbf{x})$ is the state of site $\mathbf{x} \in \mathcal{L}$, and $\mathbf{A}^t(\mathcal{N}_\mathbf{x}) = \left\{\mathbf{A}^t(\mathbf{n}) : \mathbf{n} \in \mathcal{N}_\mathbf{x}\right\}$ is the state collection over the site's neighborhood $\mathcal{N}_\mathbf{x} = \{\mathbf{x} + \mathbf{n} : \mathbf{n} \in \mathcal{N}\}$. The *global rule* is

$\Phi : S^{\mathcal{L}} \to S^{\mathcal{L}}$ such that $\Phi(\mathbf{A})(\mathbf{x}) = \phi(\mathbf{A}(\mathcal{N}_{\mathbf{x}}))$. Starting from an initial configuration $\mathbf{A}^0$, the grid is updated according to the global rule Φ for each time step Δt, leading to the following time evolution:

$$\Phi(\mathbf{A}^0) = \mathbf{A}^{\Delta t}, \Phi(\mathbf{A}^{\Delta t}) = \mathbf{A}^{2\Delta t}, \ldots, \Phi(\mathbf{A}^t) = \mathbf{A}^{t+\Delta t}, \ldots. \tag{1}$$

After N repeated updates (or *generations*):

$$\Phi^N(\mathbf{A}^t) = \mathbf{A}^{t+N\Delta t}. \tag{2}$$

2.1.1 Definition of Game of Life

Take GoL as an example, $\mathcal{A}_{\text{GoL}} = (\mathcal{L}, \mathcal{T}, \mathcal{S}, \mathcal{N}, \phi)$, where $\mathcal{L} = \mathbb{Z}^2$ is the two-dimensional discrete grid, $\mathcal{T} = \mathbb{Z}$ is the discrete timeline, $\mathcal{S} = \{0, 1\}$ is the singular state set, and $\mathcal{N} = \{-1, 0, 1\}^2$ is the Moore neighborhood (Chebyshev L^∞ norm) including the site itself and its eight neighbors (Figure 2(a)).

The totalistic neighborhood sum of site $\mathbf{x}$ is:

$$\mathbf{S}^t(\mathbf{x}) = \sum_{n \in \mathcal{N}} \mathbf{A}^t(\mathbf{x} + \mathbf{n}). \tag{3}$$

Every site is updated synchronously according to the local rule:

$$\mathbf{A}^{t+1}(\mathbf{x}) = \begin{cases} 1 & \text{if } \mathbf{A}^t(\mathbf{x}) = 0 \text{ and } \mathbf{S}^t(\mathbf{x}) \in \{3\} \ (\text{birth}) \\ 1 & \text{if } \mathbf{A}^t(\mathbf{x}) = 1 \text{ and } \mathbf{S}^t(\mathbf{x}) \in \{3, 4\} \ (\text{survival}) \\ 0 & \text{otherwise } (\text{death}). \end{cases} \tag{4}$$

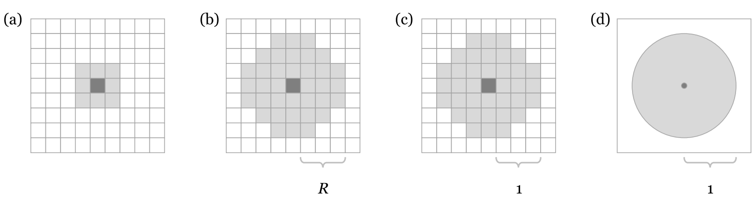

Figure 2. Neighborhoods in various CAs. (a) Eight-site Moore neighborhood in GoL. (b–d) Neighborhoods in Lenia, including (b) range R extended neighborhood, (c) its normalization in discrete Lenia and (d) the unit ball neighborhood in continuous Lenia.

2.1.2 Definition of Lenia

Discrete Lenia generalizes GoL by extending and normalizing the spacetime-state dimensions. Discrete Lenia is used for computer simulation and analysis, and with normalization, patterns from different dimensions can be compared.

The state set is extended to $\mathcal{S} = \{0, 1, 2, \ldots, P\}$ with maximum $P \in \mathbb{Z}$. The neighborhood is extended to a discrete ball (Euclidean L^2 norm) $\mathcal{N} = \mathbb{B}_R[0] = \{\mathbf{x} \in \mathcal{L} : \|\mathbf{x}\|_2 \leq R\}$ of range $R \in \mathbb{Z}$ (Figure 2(b)).

To normalize, define or redefine $R, T, P \in \mathbb{Z}$ as the *space*, *time* and *state resolutions*, and their reciprocals $\Delta x = 1 / R$, $\Delta t = 1 / T$, $\Delta p = 1 / P$ as the *site distance*, *time step* and *state precision*, respectively. The dimensions are scaled by the reciprocals (Figure 2(c)):

$$\mathcal{L} = \Delta\mathrm{x}\mathbb{Z}^2,\ \mathcal{T} = \Delta t\mathbb{Z},\ \mathcal{S} = \Delta p\{0 \ldots P\},\ \mathcal{N} = \mathbb{B}_1[0]. \tag{5}$$

Continuous Lenia is hypothesized to exist as the resolutions of discrete Lenia approach infinity $R, T, P \to \infty$ and the steps Δx, Δt, Δp become infinitesimals $\mathrm{d}x$, $\mathrm{d}t$, $\mathrm{d}p$; the dimensions will approach their continuum limits—that is, the Euclidean space, the real timeline, the unit interval states and the continuous unit ball neighborhood (Figure 2(d)):

$$\mathcal{L} = \mathbb{R}^2,\ \mathcal{T} = \mathbb{R},\ \mathcal{S} = [0, 1],\ \mathcal{N} = \mathbb{B}_1[0]. \tag{6}$$

However, there is a cardinality leap between the discrete dimensions in discrete Lenia and the continuous dimensions in continuous Lenia. The existence of the continuum limit for space was proved mathematically in [26], and our computer simulations provide empirical evidence for space and time (see Section 3.1).

2.1.3 Local Rule

To apply Lenia's local rule to every site $\mathbf{x}$ at time t, convolve the grid with a *kernel* $\mathbf{K} : \mathcal{N} \to \mathcal{S}$ to yield the *potential distribution* $\mathbf{U}^t$:

$$\mathbf{U}^t(\mathbf{x}) = \mathbf{K} * \mathbf{A}^t(\mathbf{x}) \begin{cases} \sum_{n \in \mathcal{N}} \mathbf{K}(\mathbf{n})\mathbf{A}^t(\mathbf{x} + \mathbf{n})\Delta x^2 & \text{in discrete Lenia} \\ \int_{n \in \mathcal{N}} \mathbf{K}(\mathbf{n})\mathbf{A}^t(\mathbf{x} + \mathbf{n})\mathrm{d}x^2 & \text{in continuous Lenia.} \end{cases} \tag{7}$$

Feed the potential into a *growth mapping* $G : [0, 1] \to [-1, 1]$ to yield the *growth distribution* $\mathbf{G}^t$:

$$\mathbf{G}^t(\mathbf{x}) = G(\mathbf{U}^t(\mathbf{x})). \tag{8}$$

Update every site by adding a small fraction Δt ($\mathrm{d}t$ in continuous Lenia) of the growth and clipping back to the unit range $[0, 1]$; the time is now $t + \Delta t$:

$$\mathbf{A}^{t+\Delta t}(\mathbf{x}) = \left[\mathbf{A}^t(\mathbf{x}) + \Delta t\mathbf{G}^t(\mathbf{x})\right]_0^1 \tag{9}$$

where $[n]_a^b = \min(\max(n, a), b)$ is the clip function.

2.1.4 Kernel

The kernel $\mathbf{K}$ is constructed by *kernel core* $K_c : [0, 1] \to [0, 1]$, which determines its detailed "texture," and *kernel shell* $K_s : [0, 1] \to [0, 1]$, which determines its overall "skeleton" (Figure 3(a–e)).

The kernel core K_c is any unimodal function satisfying $K_c(0) = K_c(1) = 0$ and usually $K_c(1/2) = 1$. By taking polar distance as an argument, it creates a uniform ring around the site:

$$K_c(r) = \begin{cases} \exp\left(\alpha - \dfrac{\alpha}{4r(1-r)}\right) & \text{exponential, } \alpha = 4 \\ (4r(1-r))^{\alpha} & \text{polynomial, } \alpha = 4 \\ \mathbf{1}_{\left[\frac{1}{4}, \frac{3}{4}\right]}(r) & \text{rectangular} \\ \ldots & \text{or others} \end{cases} \tag{10}$$

where $\mathbf{1}_A(r) = 1$ if $r \in A$ else 0 is the indicator function.

The kernel shell K_s takes a parameter vector $\beta = (\beta_1, \beta_2, \ldots, \beta_B) \in [0, 1]^B$ (*kernel peaks*) of size B (the *rank*) and copies the kernel core into equidistant concentric rings with peak heights β_i:

$$K_s(r; \beta) = \beta_{\lfloor Br \rfloor} K_c(\text{Br mod } 1). \tag{11}$$

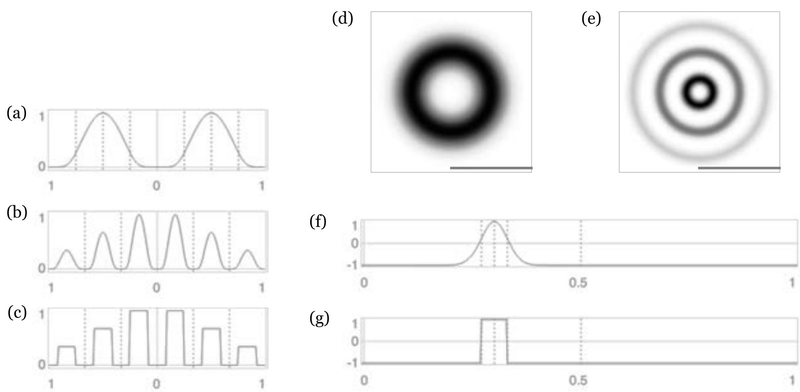

Figure 3. Core functions in Lenia. (a–c) Cross section of the kernel: kernel core $K_c(r)$ using (a) exponential function, and kernel shell $K_s(r; \beta)$ with peaks $\beta = (1, 2/3, 1/3)$ using (b) exponential or (c) rectangular core function. (d) Kernel core and (e) kernel shell as displayed in the grid, showing the "influence" (convolution weight) of the site on its neighborhood (darker = larger weight, more influence). (f–g) Growth mapping $G(u; \mu, \sigma)$ with $\mu = 0.3$, $\sigma = 0.03$ using (f) exponential or (g) rectangular function.

Finally, the kernel is normalized to make sure $\mathbf{K} * \mathbf{A} \in [0, 1]$:

$$\mathbf{K}(\mathbf{n}) = \frac{K_s(\|\mathbf{n}\|_2)}{|K_s|} \tag{12}$$

where $|K_s| = \sum_{\mathcal{N}} K_s \Delta x^2$ in discrete Lenia, or $\int_{\mathcal{N}} K_s dx^2$ in continuous Lenia.

Notes on parameter β:

- Comparing β of different ranks, a vector β is equivalent to one with n trailing zeros while space resolution R is scaled by $(B+n)/B$ at the same time, for example, $\beta = (1) \equiv (1, 0, 0)$ with R scaled by 3.
- Comparing β of the same rank, a vector β where $\forall\, i\beta_i \neq 1$ is equivalent to a scaled one $\beta / \max(\beta_i)$ such that $\exists\, i\beta_i = 1$ while the kernel remains unchanged due to normalization, for example, $\beta = (1/3, 0, 2/3) \equiv (1/2, 0, 1)$.
- Consequently, all possible β as a B-dimensional hypercube can be projected onto its $(B-1)$-dimensional hypersurfaces (see Figure 9).

2.1.5 Growth Mapping

The growth mapping $G : [0, 1] \to [-1, 1]$ is any unimodal, nonmonotonic function with parameters $\mu, \sigma \in \mathbb{R}$ (*growth center* and *growth width*) satisfying $G(\mu) = 1$ (cf., $\zeta(\cdot)$ in [23]) (Figure 3(f–g)):

$$G(u; \mu, \sigma) = \begin{cases} 2\exp\left(-\dfrac{(u-\mu)^2}{2\sigma^2}\right) - 1 & \text{exponential} \\ 2 \times \mathbf{1}_{[\mu \pm 3\sigma]}(u)\left(1 - \dfrac{(u-\mu)^2}{9\sigma^2}\right)^{\alpha} - 1 & \text{polynomial, } \alpha = 4 \\ 2 \times \mathbf{1}_{[\mu \pm \sigma]}(u) - 1 & \text{rectangular} \\ \ldots & \text{or others.} \end{cases} \tag{13}$$

2.1.6 Game of Life inside Lenia

GoL can be considered a special case of discrete Lenia with $R = T = P = 1$, using a variant of the rectangular kernel core:

$$K_c(r) = \mathbf{1}_{\left[\frac{1}{4}, \frac{3}{4}\right]}(r) + \frac{1}{2} \times \mathbf{1}_{\left[0, \frac{1}{4}\right]}(r) \tag{14}$$

and the rectangular growth mapping with $\mu = 0.35$, $\sigma = 0.07$.

2.1.7 Summary

In summary, discrete and continuous Lenia are defined as:

$$\mathcal{A}_{\mathrm{DL}} = \Big(\Delta x\, \mathbb{Z}^2, \Delta t\, \mathbb{Z}, \Delta \mathrm{p}\{0 \ldots \mathrm{P}\}, \\ \mathbb{B}_1[0], \mathbf{A}^{t+\Delta t} \mapsto \big[\mathbf{A}^t + \Delta t\, G_{\mu,\sigma}(\mathbf{K}_\beta * \mathbf{A}^t)\big]_0^1\Big) \tag{15}$$

$$\mathcal{A}_{\mathrm{CL}} = \\ \Big(\mathbb{R}^2, \mathbb{R}, [0, 1], \mathbb{B}_1[0], \mathbf{A}^{t+\mathrm{d}t} \mapsto \big[\mathbf{A}^t + \mathrm{d}t\, G_{\mu,\sigma}(\mathbf{K}_\beta * \mathbf{A}^t)\big]_0^1\Big). \tag{16}$$

The associated dimensions are: spacetime-state resolutions R, T, P; steps Δx, Δt, Δp and infinitesimals $\mathrm{d}x$, $\mathrm{d}t$, $\mathrm{d}p$. The associated parameters are: growth center μ, growth width σ and kernel peaks β of rank B. The mutable core functions are: kernel core K_c and growth mapping G.

2.2 Evolving New Species

A self-organizing, autonomous pattern in Lenia is called a *life form*, and a set of similar life forms is called a *species*. Up to the present, more than 400 species have been discovered. Interactive evolutionary computation (IEC) [33] is the major force behind the generation, mutation and selection of new species. In evolutionary computation (EC), the fitness function is usually well known and can be readily calculated. However, in the case of Lenia, due to the nontrivial task of pattern recognition, as well as aesthetic factors, evolution of new species often requires human interaction.

Interactive computer programs provide a user interface and utilities for human users to carry out mutation and selection operators manually. Mutation operators include parameter tweaking and configuration manipulation. Selection operators include observation via different views for fitness estimation (Figure 3(c–f)) and storage of promising patterns. Selection criteria include survival, long-term stability, aesthetic appeal and novelty.

Following are a few evolutionary strategies learned from experimenting and practicing.

2.2.1 Random Generation

Initial configurations with random patches of nonzero sites were generated and put into simulation using an interactive program. This is repeated using different random distributions and different parameters. Given enough time, naturally occurring life forms would emerge from the primordial soup, for example *Orbium*, *Scutium*, *Paraptera* and radial symmetric patterns (Figure 4(a)).

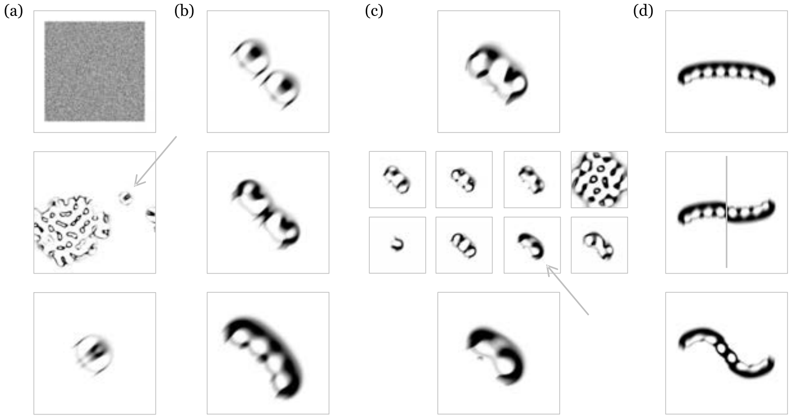

Figure 4. Strategies of evolving new Lenia life forms using IEC. (a) Random generation: random initial configuration is generated (top) and simulation is run (middle), where new life forms were spotted (arrow) and isolated (bottom). (b) Parameter tweaking: with an existing life form (top), parameters are adjusted so that new morphologies or behaviors are observed (middle, bottom). (c) Automatic exploration: a starting life form (top) is put into an automatic program to explore wide ranges of parameters (middle), where new life forms were occasionally discovered (arrow) and isolated (bottom). (d) Manual mutation: an existing life form (top) is modified, here single-side flipped (middle), and parameter tweaked to stabilize into a new species (bottom).

2.2.2 Parameter Tweaking

Using an existing life form, parameters were changed progressively or abruptly, forcing the life form to die out (explode or evaporate) or survive by changing slightly or morphing into another species. Any undiscovered species with novel structure or behavior were recorded (Figure 4(b)).

Transient patterns captured during random generation could also be stabilized into new species in this way.

Long-chain life forms (e.g., Pterifera) could first be elongated by temporarily increasing the growth rate (decrease μ or increase σ), then stabilized into new species by reversing growth. Shortening could be done in the opposite manner.

2.2.3 Automatic Exploration

Starting from an existing life form, an automatic program was used to traverse the parameter space (i.e., continuous parameter tweaking). All surviving patterns were recorded; among them new species were occasionally found. Currently, automated exploration is ineffective without the aid of artificial intelligence (e.g., pattern recognition) and has only been used for simple conditions (rank 1, mutation by parameter tweaking, selection by survival) (Figure 4(c)).

2.2.4 Manual Mutation

Patterns were edited or manipulated (e.g., enlarging, shrinking, mirroring, single-side flipping, recombining) using our interactive program or other numeric software and then parameter tweaked in an attempt to stabilize into new species (Figure 4(d)).

2.3 Analysis of Life Forms

2.3.1 Qualitative Analysis

By using computer simulation and visualization and taking advantage of the inate human ability of spatial and temporal pattern recognition, the physical appearances and movements of known species were being observed, documented and categorized, as reported in Sections 3.4 and 3.5. Using an automatic traverse program, the distributions of selected species in the parameter space were charted, as reported in Section 3.3. A set of criteria, based on the observed similarities and differences among the known species, was devised to categorize them into a hierarchical taxonomy, as reported in Section 3.2.

2.3.2 Quantitative Analysis

Statistical methods were used to analyze life forms to compensate for the limitations in human observation regarding subtle variations and long-term trends. A number of *statistical measures* were calculated over the configuration (i.e., mass distribution) $\mathbf{A}$ and the positive-growth distribution $\mathbf{G}|_{\mathbf{G}>0}$:

- *Mass* is the sum of states, $m = \int \mathbf{A}(\mathbf{x})d\mathbf{x}$; [mg]
- *Volume* is the number of positive states, $V_m = \int_{\mathbf{A}>0} dx$ [mm^2]
- *Density* is the overall density of states, $\rho_m = m / V_m$ [mg mm^{-2}]
- *Growth* is the sum of positive growth, $g = \int_{\mathbf{G}>0} \mathbf{G}(\mathbf{x})d\mathbf{x}$ [mg s^{-1}]
- *Centroid* is the center of states, $\overline{\mathbf{x}}_m = \int \mathbf{x}\mathbf{A}(\mathbf{x})d\mathbf{x} / m$
- *Growth center* is the center of positive growth, $\overline{\mathbf{x}}_g = \int_{\mathbf{G}>0} \mathbf{x}\mathbf{G}(\mathbf{x})d\mathbf{x} / g$
- *Growth-centroid distance* is the distance between the two centers, $d_{gm} = |\overline{\mathbf{x}}_g - \overline{\mathbf{x}}_m|$ [mm]
- *Linear speed* is the linear moving rate of the centroid, $s_m = |d\overline{\mathbf{x}}_m / dt|$ [mm s^{-1}]

- *Angular speed* is the angular moving rate of the centroid, $\omega_m = \mathrm{d} / \mathrm{d}t \arg(d\overline{\mathbf{x}}_m / \mathrm{d}t)$ [rad s^{-1}]
- *Mass asymmetry* is the mass difference across the directional vector, $m_\Delta = \int_{c>0} \mathbf{A}(\mathbf{x}) \mathrm{d}\mathbf{x} - \int_{c<0} \mathbf{A}(\mathbf{x}) \mathrm{d}\mathbf{x}$ [mg] where $c = \mathrm{d}\overline{\mathbf{x}}_m \times (\mathbf{x} - \overline{\mathbf{x}}_m)$
- *Angular mass* is the second moment of mass from the centroid, $I_m = \int \mathbf{A}(\mathbf{x}) (\mathbf{x} - \overline{\mathbf{x}}_m)^2 \mathrm{d}\mathbf{x}$ [mg mm^2]
- *Gyradius* is the root-mean-square of site distances from the centroid, $r_m = \sqrt{I_m / m}$ [mm]
- Others, for example, Hu's and Flusser's moment invariants ϕ_i [34, 35]

Note: Brackets indicate the units of measure borrowed from SI units in microscopic scale, for example, "mm" for length, "rad" for angle, "s" for time and "mg" for states (cf., "lu" and "tu" in [4]).

Based on the multivariate time series of statistical measures, the following "meta-measures" could be calculated:

- Summary statistics (mean, median, standard deviation, minimum, maximum, quartiles)
- Quasi period (estimated using, e.g., autocorrelation, periodogram)
- Degree of chaos (e.g., Lyapunov exponent, attractor dimension)
- Probability of survival

The following charts were plotted using various parameters, measures and meta-measures:

- Time series chart (measure vs. time)
- Phase space trajectory (measure vs. measure) (e.g., Appendix, Figure C.3 insets)
- Allometric chart (meta vs. meta) (e.g., Figure 13 and Appendix, Figure C.2)
- Cross-sectional chart (meta vs. parameter) (e.g., Appendix, Figure C.3)
- μ-σ map (parameter μ vs. σ; information as color) (e.g., Figures 8 and Appendix, Figure C.1)
- β-cube (parameter β components as axes; information as color) (e.g., Figure 9)

Over 1.2 billion measures were collected using an automatic traverse program and analyzed using numeric software like Microsoft Excel. Results are presented in Section 3.6.

2.3.3 Spatiotemporal Analysis

Constant motions like translation, rotation and oscillation render visual analysis difficult. It is desirable to separate the spatial and temporal aspects of a moving pattern so as to directly assess the static form and estimate the motion frequencies (or quasi periods).

Linear motion can be removed by *autocentering*, to display the pattern centered at its centroid $\overline{\mathbf{x}}_m$.

Using *temporal sampling*, the simulation is displayed one frame per N time steps. When any rotation is perceived as near stationary due to the stroboscopic effect, the rotation frequency is approximately the sampling frequency $f_r \approx f_s = 1 \big/ (N \Delta t)$. Calculate the sampled angular speed $\omega_s = \theta f_r = 2\pi f_r \big/ n$, where n is the number of radial symmetric axes. Angular motion can be removed by *autorotation*, to display the pattern rotated by $-\omega_s t$.

With the nontranslating, nonrotating pattern, any global or local oscillation frequency can be determined as $f_o \approx f_s$, again using temporal sampling.

3. Results

Results of the study of Lenia will be outlined in various sections: Physics, Taxonomy, Ecology, Morphology, Behavior, Physiology and Case Study.

3.1 Physics

We present general results regarding the effects of basic CA settings, akin to physics, where one studies how the spacetime fabric and fundamental laws influence matter and energy.

3.1.1 Spatial Invariance

For sufficiently fine space resolution ($R > 12$), patterns in Lenia are minimally affected by spatial similarity transformations including shift, rotation, reflection and scaling (Figure 5(d–g)). Shift invariance is shared by all homogenous CAs; reflection invariance is enabled by symmetries in neighborhood and local rule; scale invariance is enabled by large neighborhoods (as in LtL [25]); rotation invariance is enabled by circular neighborhoods and totalistic or polar local rules (as in SmoothLife [27] and Lenia). Our empirical data of near-constant metrics of *Orbium* over various space resolutions R further supports scale invariance in Lenia (Figure 6(a–b)).

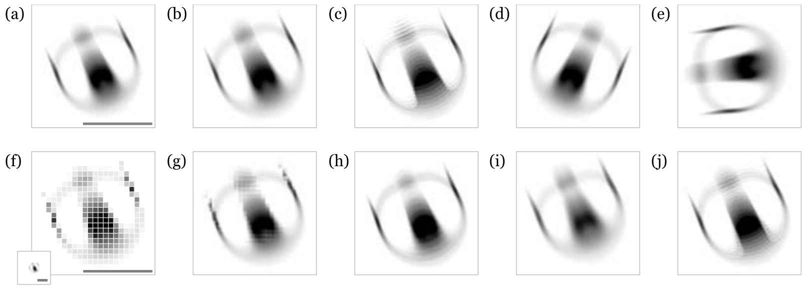

Figure 5. Plasticity of *Orbium* ($\mu = 0.15$, $\sigma = 0.016$) under various environment settings and transformations. (Scale bar is unit length = kernel radius, the same in all panels). (a) Original settings: $R = 185$, $T = 10$, $P > 10^{15}$ (double precision), exponential core functions. Core functions changed (b) to polynomial with no visible effect, (c) to rectangular produces rougher pattern. (d) Pattern flipped horizontally or (e) rotated 77° counterclockwise with no visible effect. (f) Pattern downsampled with space compressed to $R = 15$ (zoomed in, inset: actual size); (g) under recovery after upsampled using nearest-neighbor and space resolution restored to $R = 185$, eventually recovers to (a). (h) Time compressed to $T = 5$ produces rougher pattern; (i) time dilated to $T = 320$ produces smoother, lower density pattern. (j) Fewer states $P = 10$ produces rougher pattern.

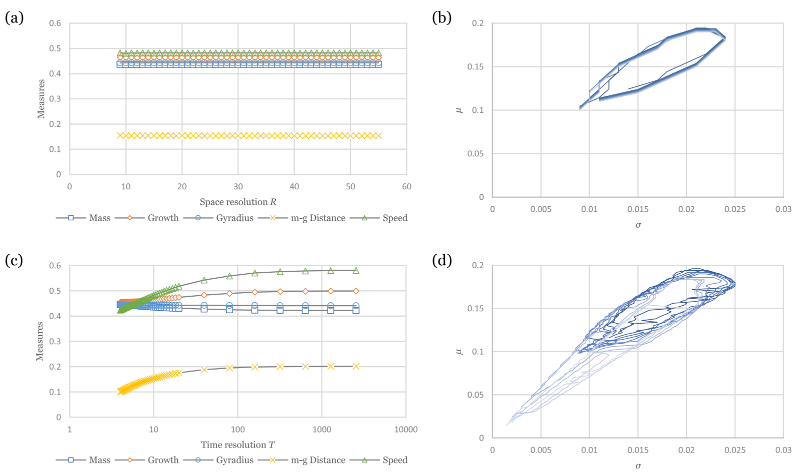

Figure 6. Effects of spacetime resolutions as experimented with *Orbium* ($\mu = 0.15$, $\sigma = 0.016$). Each data point in (a) and (c) is averaged across 300 time steps. Spatial invariance: for a range of space resolution $R \in \{9 \ldots 55\}$ and fixed time resolution $T = 10$, all statistical measures (mass m, growth g, gyradius r_m, growth-centroid distance d_{gm}, linear speed s_m) (a) remain constant and (b) the parameter range ("niche") remains static (total 557 loci). Tempo-

ral asymptosy: for a range of time resolution $T \in \{4 \ldots 2560\}$ and fixed space resolution $R = 13$, (c) structure-related measures (m, r_m) go down and dynamics-related measures (g, d_{gm}, s_m) go up, reaching each continuum limit asymptotically; (d) the parameter range expands as time dilates (dark to light enclosures, total 14 182 loci).

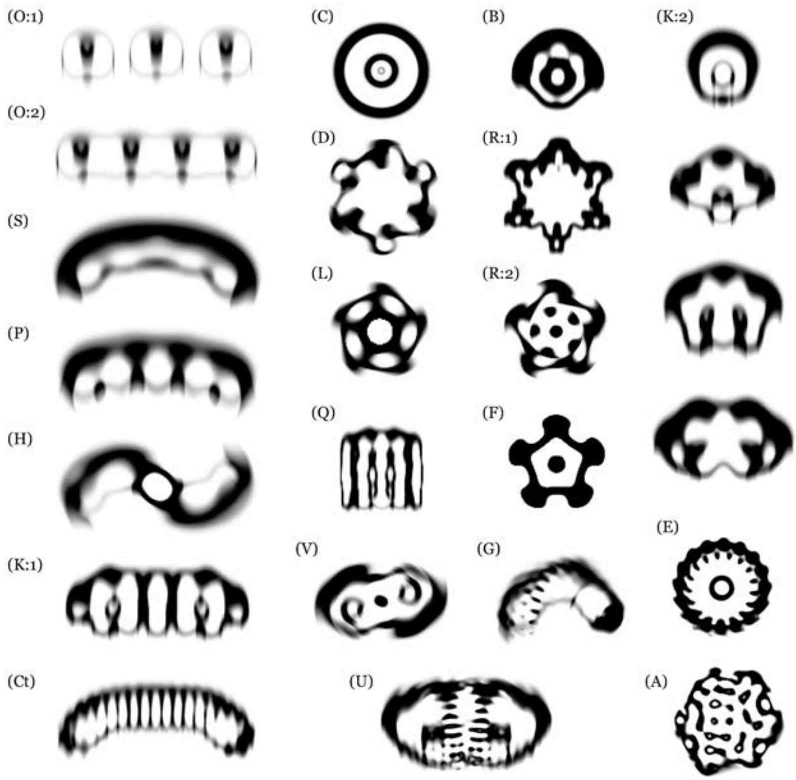

Figure 7. Biodiversity in Lenia as exemplified by the 18 Lenia families (not to scale). Column 1: (O) Orbidae, (S) Scutidae, (P) Pterifera, (H) Helicidae, (K) Kronidae, (Ct) Ctenidae. Column 2: (C) Circidae, (D) Dentidae, (L) Lapillidae, (Q) Quadridae, (V) Volvidae. Column 3: (B) Bullidae, (R) Radiidae, (F) Folidae, (G) Geminidae, (U) Uridae. Column 4: (K) Kronidae, (E) Echinidae, (A) Amoebidae.

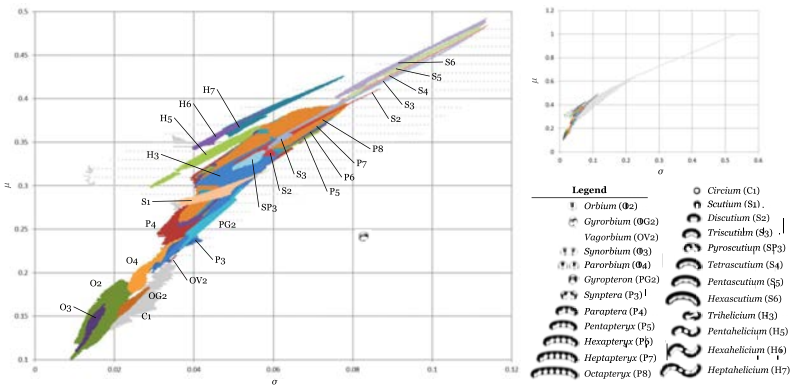

Figure 8. The μ-σ parameter space as μ-σ map, with niches of rank-1 species. Total 142 338 loci. (legend) Corresponding names and shapes for the species codes in the map. (inset) Wider μ-σ map showing the niche of *Circium* (gray region), demonstrates the four landscapes of rule space: class 1, homogenous desert (upper left); class 2, cyclic savannah (central gray); class 3, chaotic forest (lower right); class 4, complex river (central colored).

3.1.2 Temporal Asymptosy

The local rule ϕ of discrete Lenia can be considered the Euler method $\mathbf{A}_{n+1} = \mathbf{A}_n + hf(\mathbf{A}_n)$ for solving the local rule ϕ of continuous Lenia rewritten as an ordinary differential equation (ODE):

$$\mathbf{A}^{t+\mathrm{d}t} = \mathbf{A}^t + \mathrm{d}t\left[G\left(\mathbf{K} * \mathbf{A}^t\right)\right]_{-\mathbf{A}^t/\mathrm{d}t}^{\left(1-\mathbf{A}^t\right)/\mathrm{d}t} \tag{17}$$

$$\frac{\mathrm{d}}{\mathrm{d}t}\mathbf{A}^t = \left[G\left(\mathbf{K} * \mathbf{A}^t\right)\right]_{-\mathbf{A}^t/\mathrm{d}t}^{\left(1-\mathbf{A}^t\right)/\mathrm{d}t} \tag{18}$$

The Euler method should better approximate the ODE as step size h diminishes; similarly, discrete Lenia should approach its continuum limit as Δt decreases. This is supported by empirical data of asymptotic metrics of *Orbium* over increasing time resolutions T (Figure 6(c–d)) toward an imaginable "true *Orbium*" (Figure 5(i)).

3.1.3 Core Functions

Choices of kernel core K_c and growth mapping G (the core functions or "fundamental laws") usually alter the "textures" of a pattern but not its overall structure and dynamics (Figure 5(b–c)). Smoother core functions (e.g., exponential) produce smoother patterns; rougher ones (e.g., rectangular) produce rougher patterns. This plasticity suggests that similar life forms should exist in SmoothLife, which resembles Lenia with rectangular core functions, as supported by similar creatures found in both CAs (Figure 1(f–g)).

3.2 Taxonomy

We present the classification of Lenia life forms into a hierarchical taxonomy, a process comparable to the biological classification of terrestrial life [36].

3.2.1 Phylogeny of the Glider

The most famous moving pattern in GoL is the diagonally moving "glider" (Figure 1(a)). It was not until LtL [30] that scalable digital creatures were discovered, including the glider analog "bugs with stomach," and SmoothLife [27] was the first to produce an omnidirectional bug called the "smooth glider," which was rediscovered in Lenia as *Scutium* plus variants (Figure 1(e–g) left). We propose the phylogeny of the glider:

Glider → bug with stomach → smooth glider → *Scutium*.

Phylogenies of other creatures are possible, like the "wobbly glider" and *Pyroscutium* (Figure 1(f–g) right).

3.2.2 Classification

Principally, there are infinitely many types of life forms in Lenia, but a range of visually and statistically similar life forms were grouped into a *species*, defined such that one *instance* can be morphed smoothly into another by continuously adjusting parameters or other settings. Species were further grouped into higher *taxonomic ranks*—genera, families, orders, classes—with decreasing similarity and increasing generality, finally subsumed into phylum Lenia, kingdom Automata, domain Simulata and the root Artificialia. Other kinds of artificial life can potentially be incorporated into this Artificialia tree.

Following are the current definitions of the taxonomic ranks.

- A *species* is a group of life forms with the same morphology and behavior in global and local scales that form a cluster (niche) in the parameter space and follow the same statistical trends in the phase space (Figures 8 and 13). Continuous morphing among members is possible.
- A *genus* is a group of species with the same global morphology and behavior that differ locally, occupy adjacent niches and have discontinuity in statistical trends. Abrupt but reversible transformation among member species is possible.
- A *subfamily* is a series of genera with increasing number of "units" or "vacuoles" that occupy parallel niches of similar shapes.
- A *family* is a collection of subfamilies with the same architecture or body plan, composed of the same set of components arranged in similar ways.
- An *order* is a rough grouping of families with similar architectures and statistical qualities, for example, speed.

- A *class* is a high-level grouping of life forms influenced by the arrangement of the kernel.

3.3 Ecology

We describe the parameter space of Lenia ("geography") and the distribution of life forms ("ecology").

3.3.1 Landscapes

The four classes of CA rules [17, 37] correspond to the four *landscapes* in the Lenia parameter space (Figure 8):

- Class 1 (homogenous "desert") produces no global or local pattern but a homogeneous (empty) state.
- Class 2 (cyclic "savannah") produces regional, periodic immobile patterns (e.g., *Circium*).
- Class 3 (chaotic "forest") produces chaotic, aperiodic global filament network ("vegetation").
- Class 4 (complex "river") generates localized complex structures (life forms).

3.3.2 Niches

In the $(B+1)$-dimensional μ-σ-β parameter hyperspace, a life form only exists for a continuous parameter range called its *niche*. Each combination of parameters is called a *locus* (plural: loci).

For a given β, a *μ-σ map* is created by plotting the niches of selected life forms on a μ versus σ chart. Maps of rank-1 species have been extensively charted and were used in taxonomical analysis (Figure 8).

A *β-cube* is created by marking the existence (or the size of the μ-σ niche) of a life form at every β locus. As noted in Section 2.1, a B-dimensional hypercube can be reduced to its $(B-1)$-dimensional hypersurfaces, perfect for visualization in the three-dimensional case (Figure 9).

3.4 Morphology

We present the study of structural characteristics, or "morphology," of Lenia life forms in Figure 10. See Figure 7 for the family codes (O, S, P, etc.).

3.5 Behavior

We present the study of behavioral dynamics of Lenia life forms, or "ethology," in analogy to the study of animal behaviors in biology.

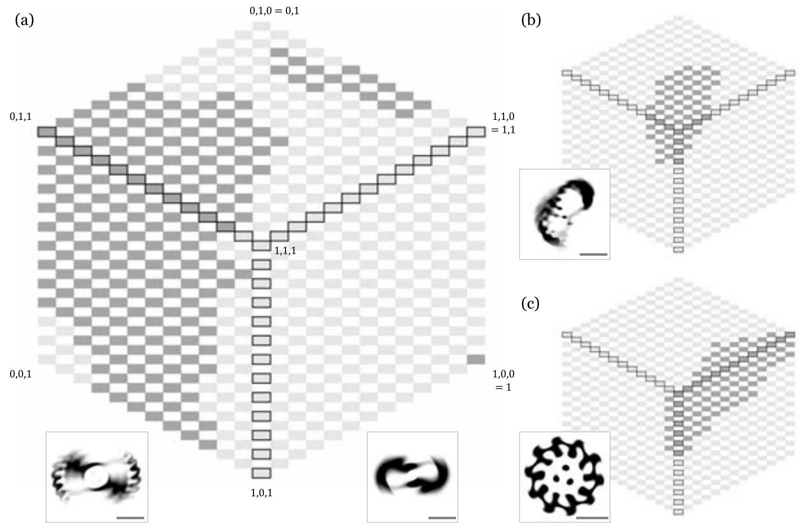

Figure 9. The β parameter space as β-cubes, with niches of selected species from the three Lenia classes. (a) β-cube of class Exokernel exemplified by *Helicium*, including rank-1 (right inset) niche at corner $(1, 0, 0)$, rank-2 (left inset) niche at edge near $(1/2, 1, 0)$ and rank-3 niche on surfaces near $(1/2, 1/2, 1)$. (b) β-cube of class Mesokernel exemplified by *Gyrogeminium gyrans* (inset), niche around $(1, 1, 1)$. (c) β-cube of class Endokernel exemplified by *Decadentium rotans* (inset), niche mostly on surface $(1, \beta_2, \beta_3)$.

3.5.1 Locomotion

In GoL, pattern behaviors include stationary (fixed, oscillation), directional (orthogonal, diagonal, rarely oblique), and infinite growth (linear, sawtooth, quadratic) [21]. SmoothLife added omnidirectional movement to the list [27]. Lenia supports a qualitatively different repertoire of behaviors, which can be described in global and local levels.

The global movements of life forms are summarized into *modes of locomotion* (Figure 11(a–c, e)):

- *Stationarity* (S) means the pattern stays still with negligible directional movement or rotation.
- *Rotation* (R) is angular movement around a stationary centroid.
- *Translocation* (T) is directional movement in a certain direction.
- *Gyration* (G) is angular movement around a noncentroid center, basically a combination of translocation and rotation.

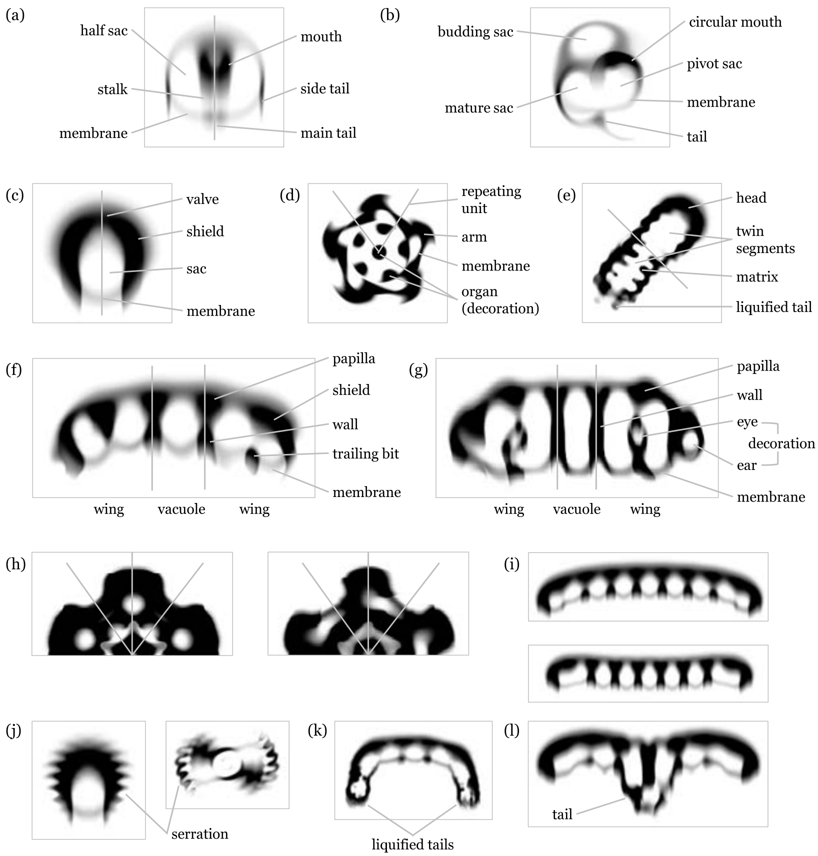

Figure 10. Anatomy and symmetries in Lenia life forms (not to scale). Simple species as standalone components: (a) *Orbium* as standalone orb; (b) *Gyrorbium* as standalone orboid wing; (c) *Scutium* as standalone scutum. Complex species: (d) radial *Asterium rotans*; (e) roughly bilateral *Hydrogeminium natans*; (f) long-chain *Pentapteryx* and (g) *Pentakronium*. (h) Symmetry of radial units: bilateral units in stationary *Asterium inversus* (left) and asymmetric units in rotational *A. torquens* (right). (i) Convexity: convex *Nonapteryx arcus* (top) and concave *N. cavus* (bottom). Ornamentation: (j) serration in higher-rank *Scutium* and *Helicium*; (k) liquefaction in *Heptageminium natans*; (l) caudation in *Octacaudopteryx*.

In formula,

$$\mathbf{A}^{t+\tau} \approx \left(S_{s\tau} \circ R_{\omega\tau}\right)\left(\mathbf{A}^{t}\right) \begin{cases} \text{Stationarity:} & s = 0, \omega = 0 \\ \text{Rotation:} & s = 0, \omega > 0 \\ \text{Translocation:} & s > 0, \omega = 0 \\ \text{Gyration:} & s > 0, \omega > 0 \end{cases} \tag{19}$$

where τ is the quasi period, S is a shift by distance $s\tau$ due to linear speed s, and R is a rotation (around the centroid) by angle $\omega\tau$ due to angular speed ω.

3.5.2 Gaits

The local details of movements are identified as different *gaits* (Figure 11(e–i)):

- *Fixation* ($_\mathrm{F}$) means negligible or no fluctuation during locomotion.
- *Oscillation* ($_\mathrm{O}$) is periodic fluctuation during locomotion.
- *Alternation* ($_\mathrm{A}$) is global oscillation plus out-of-phase local oscillations (see Section 3.6.3).
- *Deviation* ($_\mathrm{D}$) is a small departure from the regular locomotion, for example, slightly curved linear movement, slight movements in the rotating or gyrating center.
- *Chaoticity* ($_\mathrm{C}$) is chaotic, aperiodic movements.

Any gait or gait combination can be coupled with any locomotive mode and is represented by the combined code (e.g., chaotic deviated alternating translocation = T_CDA). See Table 2 for all combinations.

3.5.3 Metamorphosis

Spontaneous metamorphosis is a highly chaotic behavior in Lenia, where a “shapeshifting” species frequently switches among different morphological-behavioral *templates*, forming a continuous-time Markov chain. Each template often resembles an existing species. The set of possible templates and the transition probabilities matrix are determined by the species and parameter values (Figure 11(j)).

An extreme form of spontaneous metamorphosis is exhibited by the Amoebidae, where the structure and locomotive patterns are no longer recognizable, while a bounded size is still maintained.

These stochastic behaviors denied the previous assumption that morphologies and behaviors are fixed qualities in a species, but are actually probabilistic (albeit usually a single template with probability one).

3.5.4 Infinite Growth

Unlike the preceding behaviors where the total mass remains finite, there are behaviors associated with infinite growth (positive or negative).

Explosion or *evaporation* is uncontrolled infinite growth, where the mass quickly expands or shrinks in all directions, and the life form fails to self-regulate and dies out.

https://doi.org/10.25088/ComplexSystems.28.3.251

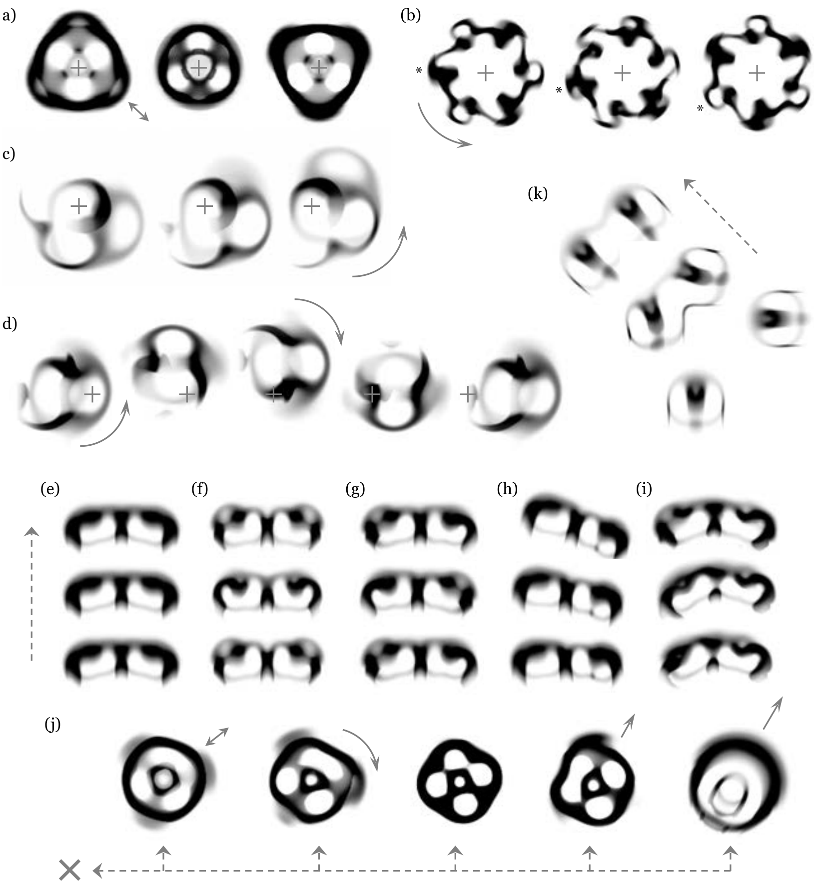

Figure 11. Behavioral dynamics in Lenia life forms (not to scale; + = reference point; → = motion; --→ = time flow, left to right if unspecified). (a) Stationarity: inverting *Trilapillium inversus* (S_O). (b) Rotation: twinkling *Hexadentium scintillans* (R_A) (* = same unit). Gyration: (c) gyrating *Gyrorbium gyrans* (G_O); (d) zigzagging *Vagorbium undulatus* (G_A). Translocation with various gaits: (e) sliding *Paraptera cavus labens* (T_F); (f) jumping *P. c. saliens* (T_O); (g) walking *P. c. pedes* (T_A); (h) deflected *P. sinus pedes* (T_{DA}); (i) chaotic *P. s. p. rupturus* (T_{CDA}). (j) Spontaneous metamorphosis: *Tetralapil lium metamorpha* switching among oscillating (S_A), rotating (R_O), frozen (S_F), walking (T_A) and wandering (T_C) (left to right), occasionally die out (×). (k) Particle reactions: two *Orbium* collide and fuse together into an intermediate, then stabilize into one *Synorbium*.

Elongation or *contraction* is controllable infinite growth, where a long-chain life form keeps lengthening or shortening in directions tangential to local segments. Microscopically, vacuoles are being constantly created or absorbed via binary fission or fusion.

Gait (type of asymmetry)	Locomotive Mode (Type of Symmetry)			
	Stationarity (Radial)	Rotation (Rotational)	Translocation (Bilateral)	Gyration (Deformed Bilateral)
fixation (static)	S_F= frozen *Pentafolium lithos*	R_F = rotating *Asterium rotans*	T_F = sliding *Paraptera cavus labens* [e]	G_F= spinning *Gyropteron serratus velox*
oscillation (dynamical)	S_O= ventilating *Hexalapillium ventilans*	R_O= torquing *Asterium torquens*	T_O = jumping *Paraptera cavus saliens* [f]	G_O = gyrating *Gyrorbium gyrans* [c]
alternation (out-of-phase)	S_A= inverting *Trilapillium inversus* [a]	R_A= twinkling *Hexadentium scintillans* [b]	T_A= walking *Paraptera cavus pedes* [g]	G_A= zigzagging *Vagorbium undulatus* [d]
deviation (unbalanced)	S_D= drifting *Octafolium tardus*	R_D= precessing *Nivium incarceratus*	T_D = deflected *Paraptera sinus pedes* [h]	G_D = revolving *Gyrorbium revolvens*
chaoticity (stochastic)	S_C = vibrating *Asterium nausia*	R_C = tumbling *Decadentium volubilis*	T_C = wandering *Paraptera s. p. rupturus* [i]	G_C = swirling *Gyrogeminium velox*

Table 2. Matrix of symmetries, asymmetries, locomotive modes and gaits. Each combination is provided with a code, a descriptive term and a sample species. (Brackets indicate subfigures in Figure 11).

As estimated by mass time series, linear and circular elongation show a linear growth rate, while spiral elongation (in Helicidae) and others shows a quadratic growth rate.

3.5.5 Particle Reactions

Using the interactive program as a "particle collider" (cf. [38]), we investigated the reactions among Orbidae (see Appendix B) instances acting as physical or chemical particles. They often exhibit elasticity and resilience during collision, engage in inelastic (sticky) collision, and seem to exert a kind of weak "attractive force" when two particles are nearby or "repulsive force" when getting too close.

Reactions of two or more *Orbium* particles with different starting positions and incident angles would result in one of the following:

- *Deflection*, two *Orbium* particles disperse in different angles.
- *Reflection*, one *Orbium* particle is unchanged and one goes in the opposite direction.
- *Absorption*, only one *Orbium* particle survives.
- *Annihilation*, both *Orbium* particles evaporate.
- *Detonation*, the resultant mass explodes into infinite growth.

- *Fusion*, multiple *Orbium* particles fuse together into Synorbinae (Figure 11(k)).
- *Parallelism*, multiple *Orbium* particles travel in parallel with "forces" subtly balanced, forming Parorbinae (Figure 7(O:1)).

Starting from a composite Orbidae may result in:

- *Fission*, one Synorbinae breaks into multiple Synorbinae or *Orbium* particles.

3.6 Physiology

The exact mechanisms of morphogenesis (self-organization) and homeostasis (self-regulation), or "physiology," in Lenia are not well understood. Here we present a few observations and speculations.

3.6.1 Symmetries and Behaviors

A striking result in analyzing Lenia is the correlations between structural symmetries/asymmetries (Appendix B.5) and behavioral dynamics (Section 3.5).

At a global scale, the locomotive modes (stationarity, rotation, translocation, gyration) correspond to the types of overall symmetry (radial, rotational, bilateral, deformed bilateral). At a local scale, the locomotive gaits (fixation, oscillation, alternation, deviation, chaoticity) correspond to the development and distribution of asymmetry (static, dynamic, out-of-phase among units, unevenly distributed, stochastic development) (Table 2).

3.6.2 Stability-Motility Hypothesis

A closer look at these symmetry-behavior (see Appendix B.5) correlations suggests the mechanisms of how motions arise.

In a bilateral species, while there is lateral (left-right) reflectional symmetry, the heavy asymmetry along the longitudinal (rostrocaudal) axis may be the origin of directional movement. In a deformed bilateral species, the lateral symmetry is broken, thus introduces an angular component to its linear motion.

In a radial species, bilateral repeating units are arranged radially, and all directional vectors cancel out, thus overall remain stationary. In a rotational species, asymmetric repeating units mean the lateral symmetry is broken, thus initiates angular rotation around the centroid.

On top of these global movements, the dynamical qualities of asymmetry—static/dynamical, in-phase/out-of-phase, balanced/unbalanced, regular/stochastic—lead to the dynamical qualities of locomotion (i.e., gaits).

Based on this reasoning, we propose the *stability-motility hypothesis* (potentially applicable to real-world physiology or evolutionary biology):

> Symmetry provides stability; asymmetry provides motility.
>
> Distribution of asymmetry determines locomotive mode; its development determines gait.

3.6.3 Alternation and Internal Communication

The alternation gait, that is, global oscillation plus out-of-phase local oscillations, is one of the most complicated behaviors in Lenia. It demonstrates phenomena like long-range synchronization and rotational clockwork.

Alternating translocation (T_A) in a simple bilateral species, where the two halves are in opposite phases, is the spatiotemporal reflectional (i.e., glide) symmetry at half-cycle, in addition to the full oscillation:

$$\mathbf{A}^{t+\frac{\tau}{2}} \approx \left(S_{\frac{s\tau}{2}} \circ F\right)\left(A^t\right) \tag{20}$$

$$\mathbf{A}^{t+\tau} \approx S_{s\tau}\left(\mathbf{A}^t\right) \tag{21}$$

where τ is the quasi period, S is a shift, and F is a flip (Figure 11(g)).

Alternating long-chain species, where two wings are oscillating out of phase but the main chain remains static, demonstrate *long-range synchronization* in which faraway structures are able to synchronize. We performed experiments to show that alternation is self-recovering, meaning that it is not coincidental but actively maintained by the species.

Alternating gyration (G_A) is a special case in *Vagorbium* (a variant of *Gyrorbium*) where it gyrates to the opposite direction every second cycle, resulting in a zigzag trajectory (Figure 11(d)).

Alternating stationarity (S_A) occurs in stationary radial life forms (with n repeating units) and leads to spatiotemporal reflectional (or rotational) symmetry at half-cycle:

$$\mathbf{A}^{t+\frac{\tau}{2}} \approx F\left(\mathbf{A}^t\right) \approx R_{\frac{\pi}{n}}\left(\mathbf{A}^t\right) \tag{22}$$

$$\mathbf{A}^{t+\tau} \approx \mathbf{A}^t \tag{23}$$

where R is a rotation. This gives an optical illusion of “inverting” motions (Figure 11(a)).

Alternating rotation (R_A) is an intricate phenomenon found in rotational species, especially family Dentidae. Consider a Dentidae species with n repeating units; two adjacent units are separated spatially by angle $2\pi/n$ and temporally by k/n cycle, $k \in \mathbb{Z}$ (Figure 12). After

$1/n$ cycle, the pattern recreates itself with rotation due to angular speed ω, plus an extra spatiotemporal rotational symmetry of m units due to pattern alternation, $m \in \mathbb{Z}$:

$$\mathbf{A}^{t+\frac{\tau}{n}} \approx R_{\frac{\omega\tau}{n}+\frac{2\pi m}{n}}\left(\mathbf{A}^t\right) \tag{24}$$

$$\mathbf{A}^{t+\tau} \approx R_{\omega\tau}\left(\mathbf{A}^t\right). \tag{25}$$

This gives an illusion that local features (e.g., a hole) are transferring from one unit to another (Figure 12 outer arrows). The values of k, m seem to follow some particular trend (Table 3).

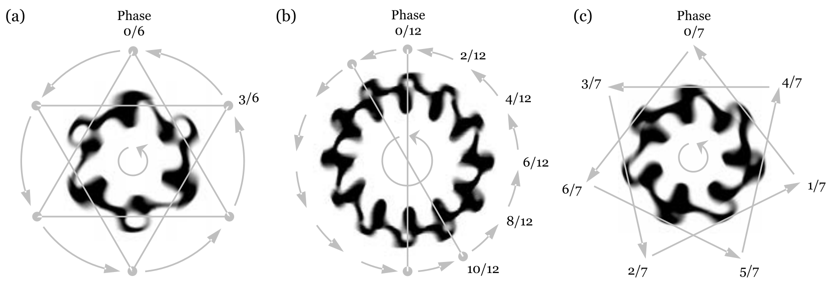

Figure 12. "Rotational clockwork" in selected alternating Dentidae species. After $1/n$ cycle, all phases advance by $1/n$ while phase relations remain unchanged (not to scale; → = phase transfer; ⊸ = same phase; ↺ = rotation, taken as the positive direction). (a) Even-sided *Hexadentium scintillans*, with opposite-phase adjacent units and same-phase alternating units. (b) Even-sided *Dodecadentium scintillans*, with sequentially out-of-phase adjacent units and same-phase opposite units. (c) Odd-sided *Heptadentium scintillans*, with globalized phase distribution.

Genus (Species *scintillans*)	Rank (B)	Units (n)	Phase Difference (k/n Cycle) of Adjacent Units	Rotational Symmetry (m units = angle $m\cdot 2\pi/n$) between $1/n$ Cycle
Hexadentium [a]	2	6	3/6	$1\cdot 2\pi/6$ (adjacent)
Heptadentium [c]	2	7	4/7	$2\cdot 2\pi/7$ (skipping)
Octadentium	2	8	4/8	$1\cdot 2\pi/8$ (adjacent)
Nonadentium	2	9	5/9	$2\cdot 2\pi/9$ (skipping)
Decadentium	4	10	2/10	$1\cdot 2\pi/10$ (adjacent)
Undecadentium	4	11	2/11	$6\cdot 2\pi/11$ (skipping)
Dodecadentium [b]	4	12	2/12	$1\cdot 2\pi/12$ (adjacent)
Tridecadentium	4	13	3/13	$9\cdot 2\pi/13$ (skipping)

Table 3. Alternation characteristics (B, n, k, m) in selected alternating Dentidae species. (Brackets indicate subfigures in Figure 12).

3.6.4 Allometry

Besides direct observation, Lenia patterns were studied through statistical measurement and analysis, akin to "allometry" in biology.

Various behaviors were found related to the average (mean or median), variability (standard deviation or interquartile length) or phase space trajectory of various statistical measures (Table 4).

A few general trends were deduced from allometric charts; for example, linear speed is found to be roughly inverse proportional to density. From the linear speed s_m versus mass m chart (Figure 13), genera form strata according to linear speed (O>P>S>H>C), and species form clusters according to mass.

Locomotion Modes and Gaits	Measure of Linear Motion (s_m)	Measure of Angular Motion ($\lvert m_\Delta \rvert$, ω_m, ω_s, …)	Measure of Oscillation (m, g, s_m, …)
stationarity	average ≈ 0	average ≈ 0	
rotation	average ≈ 0	average > 0 †	
translocation	average > 0	average ≈ 0	
gyration	average > 0	average > 0 *	
fixation			variability ≈ 0
oscillation			variability > 0
alternating translocation		variability > 0	
deviated translocation		average > 0 *	
chaoticity		⟵ chaotic trajectory ⟶	

Table 4. Allometric relationships between behavior and statistical measures. (* Deviated translocation is similar to gyration; † only works in some cases.)

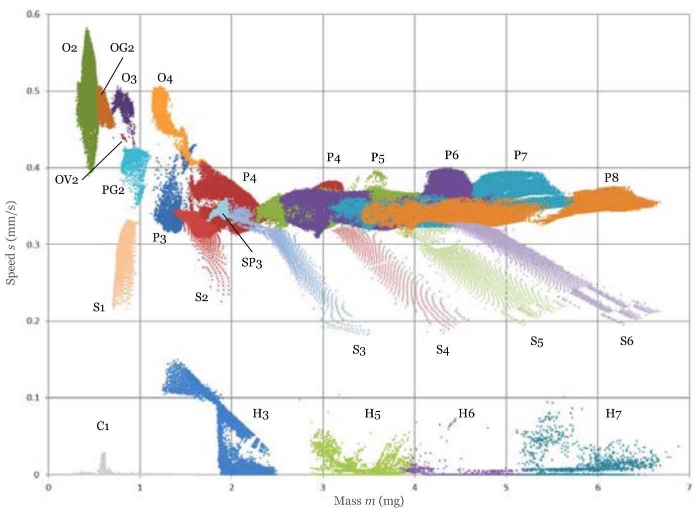

Figure 13. Allometric chart of linear speed s_m versus mass m for rank-1 species. Total 142 338 loci, 300 time steps ($t = 30$s) per locus. See Figure 8 legend for species codes.

4. Discussion

4.1 Geometric Cellular Automata

Standard CAs like GoL and ECA consider only the nearest sites as neighborhood, yet more recent variants like LtL, SmoothLife and discrete Lenia have extended neighborhoods that enable control over the "granularity" of space. The latter ones are still technically discrete, but are approximating another class of continuous systems called Euclidean automata (EA) [26]. We call them *geometric cellular automata* (GCAs). GCAs and standard CAs are fundamentally different in a number of contrasting qualities (Table 5). LtL is somehow in-between, having qualities from both sides (see Table 1).

Additionally, in standard CAs, most of the interesting patterns are concentrated in specific rules like GoL, but GCAs' patterns are scattered over the parameter space. Also, the "digital" versus "analog" distinction goes beyond a metaphor, in that many of the standard CAs are capable of "digital" universal computation, while whether a certain kind of "analog computing" is possible in GCAs remains to be seen.

As GCAs are approximants of EAs, these contrasting qualities may well exist between the truly continuous EAs and discrete CAs.

Standard CAPatterns (e.g., GoL, ECA)		Geometric CA Patterns (e.g., SmoothLife, Lenia)
	Structure	
"digital"		"analog"
nonscalable		scalable
quantized		smooth
localized motifs		geometric manifolds
complex circuitry		complex combinatorics
	Dynamics	
deterministic		unpredictable
precise		fuzzy
strictly periodic		quasi periodic
machine-like		lifelike
	Sensitivity	
fragile		resilient
mutation sensitive		mutation tolerant
rule-specific		rule-generic
rule-change sensitive		rule-change adaptive

Table 5. Contrasting qualities in standard and geometric CAs.

4.2 Nature of Lenia

Here we deep dive into the very nature of Lenia patterns, regarding their unpredictability, fuzziness, quasi periodicity, resilience and life-likeness, at times using GoL for contrast.

4.2.1 Persistence

GoL patterns are either persistent, guaranteed to follow the same dynamics every time, or temporary, eventually stabilize as persistent patterns or vanish. Lenia patterns, on the other hand, have various types of *persistence*:

1. Transient: only last for a short period.
2. Quasi stable: able to sustain for a few to hundreds of cycles.
3. Stable: survive as long as simulations went, possibly forever.
4. Metastable: stable but transform into another pattern after slight perturbations.
5. Chaotic: "walk a thin line" between chaos and self-destruction.
6. Markovian: shapeshift among templates; each has its own type of persistence.

Given a pattern, it is *unpredictable* which persistent type it belongs to unless we put it into simulation for a considerable (potentially infinite) amount of time, a situation akin to the halting problem and the undecidability in class 4 CAs [39]. This uncertainty results in the vague boundaries of niches (see Appendix, Figure C.1).

Even for a stable persistent pattern, in contrast to the GoL "glider" that will forever move diagonally, we can never be 100% sure that an *Orbium* will not eventually die out.

4.2.2 Fuzziness

No two patterns in Lenia are the same; there are various kinds of fuzziness and subtle varieties. Within a species, slightly different parameter values, rule settings or initial configurations would result in slightly different patterns (see Figure 5). Even during a pattern's lifetime, no two cycles are the same.

Consider the phase space trajectories of recurrent patterns (Figure 14): every trajectory corresponds to an attractor (or a strange attractor if chaotic). Yet, behind a group of similar patterns, there seems to be another kind of "attractor" that draws them into a common morphological-behavioral template.

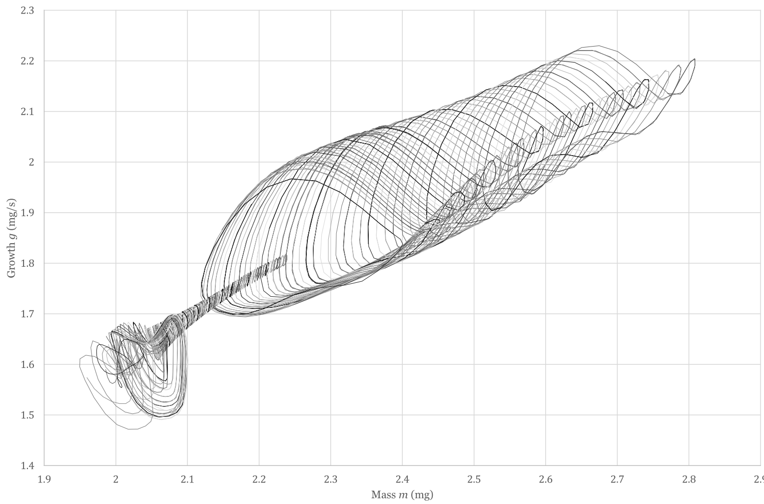

Figure 14. Phase space trajectories of growth g versus mass m (same cross section as Appendix, Figure C.3); trajectories separated by $\Delta\sigma = 0.0001$, each over a period of $t = 20$s. Each trajectory corresponds to an attractor; a group of similar trajectories hints at a species-level "attractor."

Essentialism in Western philosophy proposes that every entity in the world can be identified by a set of intrinsic features or an "essence," be it an ideal form (Plato's idealism) or a natural kind (Aristotle's hylomorphism). In Lenia, is there a certain kind of "Orbium-ness" inside all instances and occurrences of *Orbium*? Could this be identified or utilized objectively and quantitatively?

4.3 Connections with Biological Life

Besides the superficial resemblance, Lenia life may have deeper connections to biological life.

4.3.1 Symmetry and Locomotion

Both Lenia and Earth life exhibit structural symmetry and similar symmetry-locomotion relationships (Figure 15(b–c)).

Radial symmetry is universal in Lenia order Radiiformes. In biological life, radial symmetry is exhibited in microscopic protists (diatoms, radiolarians) and primitive animals historically grouped as Radiata (jellyfish, corals, comb jellies, echinoderm adults). These radiates are sessile, floating or slow-moving; similarly, Lenia radiates are usually stationary or rotating with little linear movement.

Bilateral symmetry is the most common in Lenia. In biological life, the group Bilateria (vertebrates, arthropods, mollusks, various "worm" phyla) with the same symmetry are the most successful branch of animals since the rapid diversification and proliferation near the Cambrian explosion 542 million years ago [40]. These bilaterians are optimized for efficient locomotion, and similarly, Lenia bilaterians engage in fast linear movements.

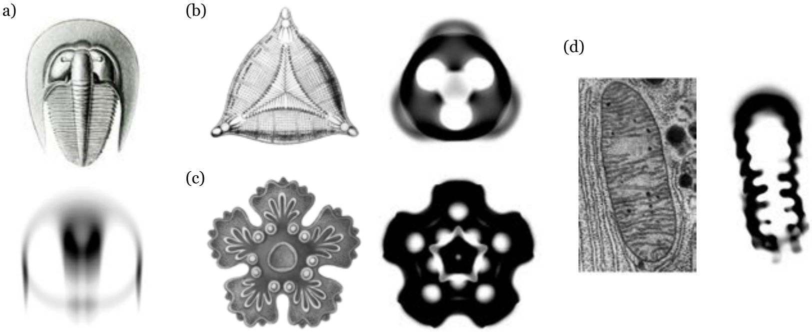

Figure 15. Appearance similarities between Earth and Lenia life. (a) Bilateral trilobite *Bohemoharpes ungula* [41, plate 47] and Lenian *Orbium bicaudatus*. (b) Trimerous diatom *Triceratium moronense* [41, plate 4] and Lenian *Trilapillium inversus*. (c) Pentamerous larva of sea star *Asterias* species [41, plate 40] and Lenian *Asterium inversus*. (d) Weakly bilateral mitochondrion [42] and Lenian *Hydrogeminium natans*, with matrix-like internal structures.

4.3.2 Adaptation to Environment

The parameter space of Lenia, earlier visualized as a geographical landscape (Section 3.3), can also be thought of as an *adaptive landscape*. Species niches correspond to fitness peaks and indicate successful adaptation to the ranges of parameters.

Any body plan (corresponds to Earth animal phylum or Lenia family) would be considered highly adaptive if it has high biodiversity, wide ecological distribution or great complexity. On Earth, the champions are the insects (in terms of biodiversity), the nematodes (in terms of ecosystem breadth and individual count) and the mammals (producing intelligent species like cetaceans and primates). In Lenia, family Pterifera is the most successful in class Exokernel in terms of diversity, niche area and complexity.

The parallels between the two systems regarding adaptability may provide insights in evolutionary biology and evolutionary computation.

4.3.3 Species Problem

One common difficulty encountered in the studies of Earth and Lenia life is the precise definition of a "species," or the *species problem*. In evolutionary biology, there exist several species concepts [43]:

- Morphological species: based on phenotypic differentiation [44]
- Phenetic species: based on numerical clustering (cf., phenetics) [45]
- Genetic species: based on genotypic clustering [46]
- Biological species: based on reproductive isolation [47]
- Evolutionary species: based on phylogenetic lineage divergence [48, 49]
- Ecological species: based on niche isolation [50]

Similar concepts are used in combination for species identification in Lenia, including morphological (similar morphology and behavior), phenetic (statistical cluster) and ecological (niche cluster) species. However, species concepts face problems in some situations, for example, in Earth's case, species aggregates or convergent evolution, and in Lenia's case, niche complex or shapeshifting life forms. It remains an open question whether clustering into species and grouping into higher taxa can be carried out objectively and systematically.

5. Online Resources

- Appendix
  wpmedia.wolfram.com/uploads/sites/13/2019/10/28-3-1-Appendix.pdf
  A: Computer Implementation
  B: More Results
  C: Case Study
  D: More on the Nature of Lenia
  E: Future Work
- Showcase video of Lenia at https://vimeo.com/277328815.
- Source code of Lenia at http://github.com/Chakazul/Lenia.
- Source code of Primordia at http://github.com/Chakazul/Primordia.

Acknowledgments

I would like to thank David Ha, Sam Kriegman, Tim Hutton, Kyrre Glette, Pierre-Yves Oudeyer, Lana Sinapayen and the anonymous reviewer for valuable discussions, suggestions and insights.

References

[1] M. A. Bedau, J. S. McCaskill, N. H. Packard, S. Rasmussen, C. Adami, D. G. Green, T. Ikegami, K. Kaneko and T. S. Ray, "Open Problems in Artificial Life," *Artificial Life*, **6**(4), 2000 pp. 363–376. doi:10.1162/106454600300103683.

[2] H. Sayama, "Swarm Chemistry," *Artificial Life*, **15**(1), 2009 pp. 105–114. doi:10.1162/artl.2009.15.1.15107.

[3] T. Schmickl, M. Stefanec and K. Crailsheim, "How a Life-Like System Emerges from a Simple Particle Motion Law," *Scientific Reports*, **6**, 2016 37969. doi:/10.1038/srep37969.

[4] R. P. Munafo, "Stable Localized Moving Patterns in the 2-D Gray–Scott Model." arxiv.org/abs/1501.01990.

[5] M. Gardner, "Mathematical Games: The Fantastic Combinations of John H. Conway's New Solitaire Game 'Life'," *Scientific American*, **223**(4), 1970 pp. 120–123. www.jstor.org/stable/24927642.

[6] S. Wolfram, "Statistical Mechanics of Cellular Automata," *Reviews of Modern Physics*, **55**(3), 1983 pp. 601–644. doi:10.1103/RevModPhys.55.601.

[7] K. Sims, "Evolving 3D Morphology and Behavior by Competition," *Artificial Life*, **1**(4), 1994 pp. 353–372. doi:10.1162/artl.1994.1.4.353.

[8] N. Cheney, R. MacCurdy, J. Clune and H. Lipson, "Unshackling Evolution: Evolving Soft Robots with Multiple Materials and a Powerful Generative Encoding," in *Proceedings of the 15th Annual Conference on Genetic and Evolutionary Computation (GECCO '13)*, Amsterdam, Netherlands, 2013, New York: ACM, 2013 pp. 167–174. doi:10.1145/2463372.2463404.

[9] S. Kriegman, N. Cheney and J. Bongard, "How Morphological Development Can Guide Evolution," *Scientific Reports*, **8**(1), 2018 13934. doi:10.1038/s41598-018-31868-7.

[10] M. S. Dodd, D. Papineau, T. Grenne, J. F. Slack, M. Rittner, F. Pirajno, J. O'Neil and C. T. S. Little, "Evidence for Early Life in Earth's Oldest Hydrothermal Vent Precipitates," *Nature*, **543**(7643), 2017 pp. 60–64. doi:10.1038/nature21377.

[11] D. E. Koshland Jr., "The Seven Pillars of Life," *Science*, **295**(5563), 2002 pp. 2215–2216. doi:10.1126/science.1068489.

[12] C. P. McKay, "What Is Life—and How Do We Search for It in Other Worlds?," *PLoS Biology*, **2**(9), 2004 e302. doi:10.1371/journal.pbio.0020302.

[13] D. Sagan, L. Margulis and C. Sagan. "Life." Encyclopedia Britannica. www.britannica.com/science/life.

[14] E. Schrödinger, *What Is Life? The Physical Aspect of the Living Cell & Mind and Matter*, New York: Cambridge University Press, 1967.

[15] E. O. Wilson, *Biophilia*, Cambridge, MA: Harvard University Press, 1984.

[16] C. G. Langton, "Studying Artificial Life with Cellular Automata," *Physica D: Nonlinear Phenomena*, **22**(1–3), 1986 pp. 120–149. doi:10.1016/0167-2789(86)90237-X.

[17] S. Wolfram, *A New Kind of Science*, Champaign, IL: Wolfram Media, Inc., 2002.

[18] J. von Neumann, "The General and Logical Theory of Automata," *Cerebral Mechanisms in Behavior; The Hixon Symposium* (L. A. Jeffress, ed.), New York: Wiley, 1951 pp. 1–41.

[19] S. Ulam, "On Some Mathematical Problems Connected with Patterns of Growth of Figures," in *Proceedings of Symposia in Applied Mathematics, Vol. 14*, (R. E. Bellman, ed.), Providence, RI: American Mathematical Society, 1962 pp. 215–224.

[20] A. Adamatzky, ed., *Game of Life Cellular Automata*, New York: Springer, 2010.

[21] ConwayLife.com. "LifeWiki, the Wiki for Conway's Game of Life." (Aug 29, 2019) www.conwaylife.com/wiki/Main_Page.

[22] P. Rendell, "Turing Universality of the Game of Life," in *Collision-Based Computing* (A. Adamatzky, ed.), London: Springer, 2002 pp. 513–539. doi:10.1007/978-1-4471-0129-1_18.

[23] B. MacLennan, *Continuous Spatial Automata*, Technical report CS-90-121, Department of Computer Science, University of Tennessee, Knoxville, TN, 1990.

[24] D. Griffeath, "Self-Organization of Random Cellular Automata: Four Snapshots," *Probability and Phase Transition* (G. Grimmett, ed.), Dordrecht: Springer, 1994 pp. 49–67. doi:10.1007/978-94-015-8326-8_4.

[25] K. M. Evans, "Larger than Life: Digital Creatures in a Family of Two-Dimensional Cellular Automata," in *Discrete Mathematics and Theoretical Computer Science Proceedings, Vol. AA*, 2001 pp. 177–192. www.emis.ams.org/journals/DMTCS/pdfpapers/dmAA0113.pdf.

[26] M. Pivato, "RealLife: The Continuum Limit of Larger than Life Cellular Automata," *Theoretical Computer Science*, **372**(1), 2007 pp. 46–68. doi:10.1016/j.tcs.2006.11.019.

[27] S. Rafler, "Generalization of Conway's "Game of Life" to a Continuous Domain—SmoothLife." arxiv.org/abs/1111.1567.

[28] R. P. Munafo, "Catalog of Patterns at $F = 0.0620$, $k = 0.0609$." (Aug 29, 2019) mrob.com/pub/comp/xmorphia/catalog.html.

[29] H. Sayama, "Swarm Chemistry Homepage: Sample Recipes." (Aug 29, 2019) bingweb.binghamton.edu/~sayama/SwarmChemistry/#recipes.

[30] K. M. Evans, "Larger than Life: Threshold-Range Scaling of Life's Coherent Structures," *Physica D: Nonlinear Phenomena*, **183**(1–2), 2003 pp. 45–67. doi:10.1016/S0167-2789(03)00155-6.

[31] T. J. Hutton. *SmoothLifeL Glider Closeup* [Video]. (Aug 30, 2019) www.youtube.com/watch?v=IJO-DETel0M.

[32] B. Berger. *Big Wobbly Glider in SmoothLife* [Video]. (Aug 30, 2019) www.youtube.com/watch?v=AsUtQgKuZfo.

[33] H. Takagi, "Interactive Evolutionary Computation: Fusion of the Capabilities of EC Optimization and Human Evaluation," *Proceedings of the IEEE*, **89**(9), 2001 pp. 1275–1296. doi:10.1109/5.949485.

[34] M.- K. Hu, "Visual Pattern Recognition by Moment Invariants," *IRE Transactions on Information Theory*, **8**(2), 1962 pp. 179–187. doi:10.1109/TIT.1962.1057692.

[35] J. Flusser, "Moment Invariants in Image Analysis," *International Journal of Computer and Information Engineering*, **1**(11), 2007 pp. 3721–3726. waset.org/publications/8899.

[36] C. Linnaeus, *Systema naturae per regna tria naturae, secundum classes, ordines, genera, species, cum characteribus, differentiis, synonymis, locis*, Stockholm: Impensis Direct, Laurentii Salvii, 10th ed., 1758.

[37] A. Ilachinski, *Cellular Automata: A Discrete Universe*, River Edge, NJ: World Scientific Publishing Company, 2001.

[38] G. J. Martínez, A. Adamatzky and H. V. McIntosh, "A Computation in a Cellular Automaton Collider Rule 110," *Advances in Unconventional Computing* (A. Adamatzky, ed.), Cham, Switzerland: Springer, 2017 pp. 391–428. doi:10.1007/978-3-319-33924-5_15.

[39] S. Wolfram, "Computation Theory of Cellular Automata," *Communications in Mathematical Physics*, **96**(1), 1984 pp. 15–57. doi:10.1007/BF01217347.

[40] C. R. Marshall, "Explaining the Cambrian 'Explosion' of Animals," *Annual Review of Earth and Planetary Sciences*, **34**(1), 2006 pp. 355–384. doi:10.1146/annurev.earth.33.031504.103001.

[41] E. H. P. Haeckel, *Kunstformen der Natur*, Leipzing, Vienna: Verlag des Bibliographischen Instituts, 1904. www.flickr.com/photos/biodivlibrary/albums/72157627662427009.

[42] K. Porter, "CIL:11397, Myotis lucifugus." (Aug 30, 2019) www.cellimagelibrary.org/images/11397.

[43] R. L. Mayden, "A Hierarchy of Species Concepts: The Denouement in the Saga of the Species Problem," *Species: The Units of Biodiversity* (M. F. Claridge, H. A. Dawah and M. R. Wilson, eds.), p. 381–424, New York: Chapman & Hall, 1997.

[44] C. Darwin, *On the Origin of Species*, London: John Murray, 1859.

[45] P. H. A. Sneath and R. R. Sokal, *Numerical Taxonomy, the Principles and Practice of Numerical Classification*, San Francisco: W. H. Freeman, 1973.

[46] J. Mallet, "A Species Definition for the Modern Synthesis," *Trends in Ecology & Evolution*, **10**(7), 1995 pp. 294–299. doi:10.1016/0169-5347(95)90031-4.

[47] E. Mayr, *Systematics and the Origin of Species, from the Viewpoint of a Zoologist*, New York: Columbia University Press, 1942.

[48] G. G. Simpson, “The Species Concept,” *Evolution*, **5**(4), 1951 pp. 285–298. doi:10.1111/j.1558-5646.1951.tb02788.x.

[49] W. Hennig, *Phylogenetic Systematics* (D. D. Davis and R. Zangerl, trans.), Urbana, IL: University of Illinois Press, 1966.

[50] L. Van Valen, “Ecological Species, Multispecies, and Oaks,” *Taxon*, **25**(2–3), 1976 pp. 233–239. doi:10.2307/1219444.